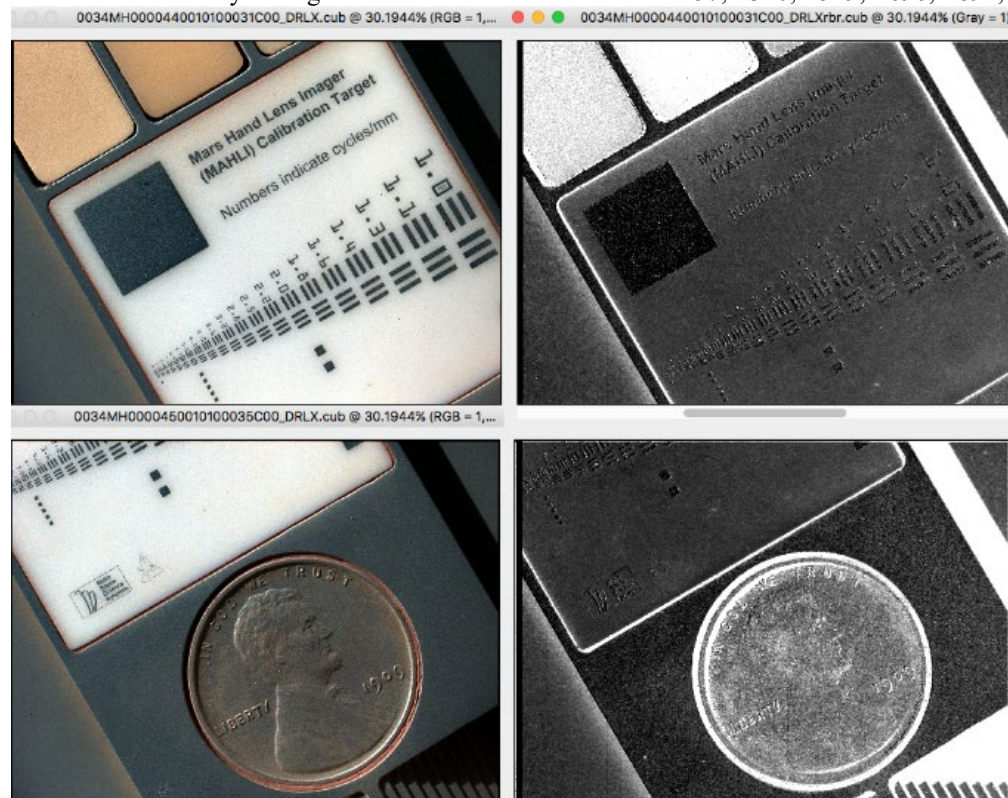


**MEASURING DUST CONTAMINATION OF THE MARS SCIENCE LABORATORY MAHLI CALIBRATION TARGET USING RED/BLUE COLOR RATIOS.** K. E. Herkenhoff<sup>1</sup>, R. A. Yingst<sup>2</sup>, and J. R. Johnson<sup>3</sup> <sup>1</sup>USGS Astrogeology Science Center, 2255 N. Gemini Dr., Flagstaff, AZ 86001 (kherkenhoff@usgs.gov), <sup>2</sup>Planetary Science Institute, Tucson, AZ 85719 (yingst@psi.edu), <sup>3</sup>Applied Physics Laboratory, Laurel, MD 20723 (Jeffrey.R.Johnson@jhuapl.edu).

**Introduction:** We used images of the Mars Science Laboratory Mars Hand Lens Imager (MAHLI) calibration target acquired under various illumination conditions to study changes in dust contamination

during the rover traverse. We selected daytime images of the calibration target that were fully sunlit and taken with the LEDs off: Sols 34, 179, 411, 591, 825, 989, 1157, 1340, 1519, 1696, 1892, 2082 (during the 2018



**Figure 1.** RGB color (left) and red/blue ratio (right, stretched so that red/blue < 1.16 is black and >2.3 is white) versions of radiometrically-calibrated MAHLI images of the MAHLI calibration target, acquired on Sol 34 with illumination from upper left. Diameter of penny is 19 mm.

Experiments using simulants of Mars dust on white, grey and black substrates show that the color of thin dust coatings becomes steadily more like the red dust with increasing coating thickness [2]. We therefore use the ratio of calibrated MAHLI red band data to blue band data as a proxy for the concentration of dust on the calibration target. But, as noted above, the effect of variable diffuse illumination must be considered, as the Martian sky is redder than the Sun [3] and contributes a larger fraction of the total surface illumination at higher atmospheric opacity. The difference in the colors of sunlit and shadowed areas is visible in Fig. 1: shadowed areas at upper and lower right have higher red/blue ratios than sunlit areas. Therefore, the colors of the shadowed and un-shadowed calibration

dust storm), 2161, and 2248. Each of these 3-band (red, green, blue) images was interpolated from the original Bayer-pattern images [1]. Images were typically acquired from a standoff of 5 cm, with one centered on the resolution target and one centered on the 1909 Lincoln penny (Fig. 1). While the observational geometry was essentially identical in all of these images, the solar incidence angle and atmospheric dust opacity varied among them.

target must be measured to understand and compensate for the magnitude of this effect, as in previous studies of the IMP and Pancam calibration targets. Unfortunately, white areas on the target cannot be used for such measurements and analysis because they were imaged only when either fully illuminated or fully shadowed. However, as shown in Figure 1, the grey titanium base of the calibration target [1] was often imaged when partly shadowed.

The observed reflectance in each of the red ( $R$ ) and blue ( $B$ ) bands is the sum of the reflectance of the direct solar radiation and the scattered (ground and sky) illumination:

$$R = R_I + R_S \quad (1)$$

$$B = B_I + B_S \quad (2)$$

where the subscripts refer to the directly illuminated ( $I$ ) and scattered ( $S$ ) components. The scattered component can be estimated by measuring the brightness in shadowed areas, which includes reflections from rover hardware and the Martian surface. We are interested

in variations in dust abundance that cause changes in the red/blue ratio of directly illuminated areas, which can be approximated using equations 1 and 2:

$$\frac{R_I}{B_I} = \frac{R - R_S}{B - B_S} \quad (3)$$

This formula ignores the wavelength-dependent extinction of the direct solar illumination by dust in the Martian atmosphere, and is therefore valid only when atmospheric opacity is  $<1$ . However, the subtraction of the brightness observed in shadowed areas partly corrects for wavelength-dependent scattering.

**Data Processing and Analysis:** Radiometrically-calibrated, linearized MAHLI images [1] were converted and processed using the USGS Integrated Software for Imagers and Spectrometers (ISIS) version 3 [4]. The ISIS program “qview” was used to display images and extract data from them. Calibrated I/F was calculated for each pixel using data included in the image labels. The reflectance difference between illuminated and shadowed areas was measured near the shadow boundary, where illumination and viewing geometry is nearly identical in the illuminated and shadowed areas. Images of the calibration target were acquired at various times of day and rover orientations, so shadows appear in different parts of the various images. Shadows on and near the “staircase” at the bottom of the target are typically visible, so these were used to measure brightness profiles across shadow boundaries on various sols. The shadow boundaries are not sharp primarily because the image is slightly out of focus in those areas and partly due to the angular size of the Sun at Mars ( $0.35^\circ$ ). In addition, the aureole around the sun (due to forward scattering by suspended dust particles) causes the curvature of the reflectance plots near the shadow boundary, seen on the left side of the plot in Fig. 2.

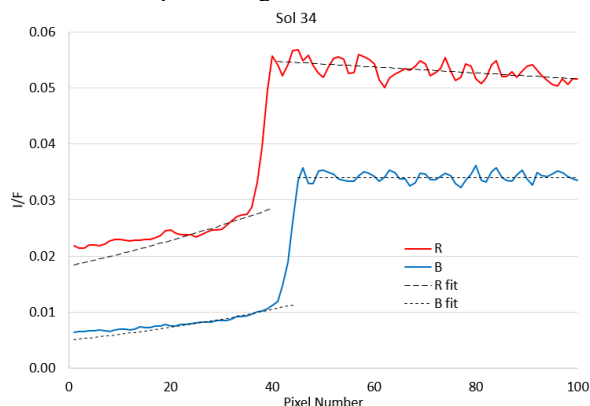


**Figure 2.** Reflectance ( $I/F$ ) profiles across shadow boundary in Sol 34 MAHLI image. The profiles are offset horizontally for clarity. The profiles in shadow were fit using data between pixel 20 and the steep rise at the edge of the shadow, so the data deeper in shadow deviate from the fits.

Red and blue reflectance profiles extracted along stair tread 3 at the bottom of a Sol 34 image show features typical of images taken later in the mission (Fig. 2). Exponential fits were used to extrapolate the  $I/F$  in the shadow to the edge of the illuminated area, where it was subtracted from linear fits of the illuminated profiles at the same location. Ranges of data were selected for fitting based on the apparent quality of the data; for example, the data deep in shadow was not as useful in modeling the rise in shadow brightness near the edge of the shadow, as illustrated in Figure 2.

**Results:** This approach described above was used to derive the corrected red/blue ratio and associated uncertainty for selected images. Changes in red/blue ratio during the MSL mission (Table 1) suggest that dust deposited on the calibration target during landing was partly removed later, consistent with changes in the appearance of the target surfaces seen in the images. Changes in the color ratio are not correlated with atmospheric opacity ( $\tau$ ), which was interpolated from 880-nm normal opacity measurements made during the MSL mission using Mastcam observations of the sun. MAHLI images of the calibration target acquired on Sols 2082 ( $\tau = 3.3$ ) and 2161 ( $\tau = 1.6$ ), during the 2018 global dust storm, could not be analyzed using the technique described above because the shadow edge was too diffuse.

**Table 1.** Corrected red/blue ratios and standard deviations for each observation. Tau ( $\tau$ ) is the interpolated 880-nm normal opacity.

Sol	Corrected R/B	$\tau$
34	$1.16 \pm 0.16$	0.74
179	$1.10 \pm 0.12$	0.98
989	$0.99 \pm 0.13$	1.07
1340	$1.05 \pm 0.17$	0.79
1519	$0.97 \pm 0.05$	0.98
1696	$0.98 \pm 0.10$	0.84
2248	$1.06 \pm 0.06$	0.77

**Conclusions:** Color reflectance data indicate that dust contamination of the MAHLI calibration target varied during the MSL mission. The target was contaminated by dust raised by the landing rockets, but this dust was partly removed later in the mission. Winds are likely to have removed some of the dust, and later dust accumulation is evident, including during the 2018 global dust storm.

**References:** [1] Edgett *et al.* (2012) *Space Sci. Rev.*, 170, 259–317. [2] Johnson, J. R. *et al.* (2006) *JGR*, 111, doi:10.1029/2005JE002658. [3] Kinch, K. M. *et al.* (2015) *Earth Space Sci.*, 2, 144–172. [4] Anderson, J. A. *et al.* (2004) *LPS XXXV*, Abstract #2039.